2013 European Control Conference (ECC)
July 17-19, 2013, Zürich, Switzerland.

State observer for a low-order plant under intrinsic pulse-modulated feedback: a case study

Alexander N. Churilov, Alexander Medvedev and Zhanybai T. Zhusubaliyev

Abstract— **Dynamical behaviors in a recently proposed observer for linear time-invariant systems under intrinsic pulse-modulated feedback are studied. A special case of scalar continuous dynamics is considered as it is not covered by the previously presented mathematical analysis. Notably, the lowest non-trivial differential order of the continuous part of the plant results in a more complex dynamics of the observer. In fact, the convergence of the observer becomes dependent on the observer initialization, which phenomenon does not exist in the case of the second and higher order continuous dynamics. As an alternative to the static gain observer, an integral feedback observer is suggested that exhibits global convergence for certain values of the observer gain and types of the periodic solution in the observed plant. Extensive bifurcation analysis is though necessary to select a proper observer gain.**

I. INTRODUCTION

A static gain observer for linear continuous plants with intrinsic pulse-modulated feedback was proposed in [1]. The problem roots in the estimation of unmeasurable hormone concentrations in hormonal axes with pulsatile secretion [2]. For an impulsive system with modulated jumps, the observer is supposed to not only drive the continuous state estimation error to zero, but also synchronize the sequence of jump instants estimated by the observer with that of the plant.

This paper presents analysis of a specialized version of the observer studied in [1], with the continuous part reduced to a first-order differential equation. The dynamics of the mathematical model that the observer is based on, but not these of the observer, were considered in [3]. The analysis in [3] has shown that such a structurally simplified system still preserves the main features of the system with a multi-dimensional continuous part and exhibits periodic solutions of high multiplicity as well as transition to chaos through a cascade of period-doubling bifurcations.

Contrary to what might be expected, it is found analytically and by bifurcation analysis that the observer for the reduced model possesses more complex dynamics than in a multidimensional case and fails to converge for some initial conditions. This paper presents an explanation to the observed phenomena as well as a way of improving the observer performance through an integrator feedback.

A. Churilov is with the Dept. of Mathematics and Mechanics, St. Petersburg State University, St.Petersburg, Russia, a_churilov@mail.ru

A. Medvedev is with the Dept. of Information Technology, Uppsala University, Uppsala, Sweden, alexander.medvedev@it.uu.se

Zh. Zhusubaliyev is with the Dept. of Computer Science, South West State University, Kursk, Russia, zhanybai@hotmail.com

A. Medvedev was in part financed by the European Research Council, Advanced Grant 247035 (SysTEAM) and Grant 2012-3153 from the Swedish Research Council.

The paper is composed as follows. First the model equations are given, mathematical properties of the model are briefly summarized, and necessary terminology is provided. Then, the observer equations are specialized to the case of a scalar continuous part and a pointwise mapping completely characterizing the observer dynamics is introduced. Further, it is demonstrated that the pointwise mapping is not continuously differentiable on certain manifolds of the state space of the hybrid system and has stability properties that depend on the initialization of the observer.

II. PLANT EQUATIONS

Consider a plant governed by the equation

$$\frac{dx}{dt} = -\lambda x, \tag{1}$$

where λ is a positive scalar and $x(t)$ is the scalar measurable state. The state $x(t)$ undergoes intrinsic (non-measurable) jumps at the time instants $t = t_n$:

$$x(t_n^+) = x(t_n^-) + \gamma_n, \tag{2}$$

$$t_{n+1} = t_n + T_n, \quad T_n = \Phi(x(t_n^-)), \quad \gamma_n = F(x(t_n^-)). \tag{3}$$

The minus and plus in the superscripts denote a left-sided and a right-sided limit, respectively. The functions $\Phi(\cdot)$ and $F(\cdot)$ are continuously differentiable, strictly monotonic and bounded with strictly positive lower bounds. The function $\Phi(\cdot)$ is increasing and the function $F(\cdot)$ is decreasing. The above assumptions imply that all the solutions of system (1)–(3) are bounded and there are no equilibria, see [2].

Obviously, the system under consideration is positive, i.e. if the initial value $x(t_0^-)$ is positive, then $x(t) > 0$ for all $t \geqslant t_0$.

To completely characterize the system dynamics, not only the continuous-time state $x(t)$, but also the jump instants t_n should be taken into account, yielding a two-dimensional hybrid system that is analyzed in detail in [3]. In fact, it constitutes a specialization of a more general model treated in [2].

The plant is subject to unknown initial conditions $(x(0),\, t_0)$ and the first firing instant of the pulsatile feedback occurs after the initial time instant, $t_0 \geqslant 0$. With regard to the hybrid system dynamics, the initial conditions are specified as $(x(t_0^-),\, t_0)$.

Define $x_n = x(t_n^-)$. Then any solution $x(t)$ of (1)–(3) satisfies the discrete-time equation

$$x_{n+1} = Q_0(x_n), \tag{4}$$

where

$$Q_0(x) = \mathrm{e}^{-\lambda\Phi(x)}(x + F(x)). \tag{5}$$

Together with the equation $t_{n+1} = t_n + \Phi(x_n)$, (4) completely defines the dynamics of (1)–(3), [2]. Once a sequence (x_n, t_n) is determined, the continuous state in between the firing times is uniquely given by

$$x(t) = \mathrm{e}^{-\lambda(t-t_n)}(x_n + F(x_n)), \qquad t_n < t < t_{n+1}.$$

Proposition 1 ([3]): The map given by (5) always has a unique fixed point $x > 0$. The derivative of map (5) satisfies $Q_0'(x) < 1$ for any $x \geqslant 0$.

Consider periodic solutions of (4), and, consequently, of (1)–(3). A set of points $S(x_0) = \{x_0,\ x_1, \ldots\}$ with $x_{n+1} = Q_0(x_n)$ is usually termed as *an orbit* of system (4) through the point x_0.

A solution $x_n, n = 0, 1, \ldots$ is called m-periodic (for some $m \geqslant 1$), if m is the smallest value for which the relationships

$$x_1 = Q_0(x_0), \quad x_2 = Q_0(x_1), \quad \ldots,$$
$$x_m = Q_0(x_{m-1}), \quad x_m = x_0$$

hold. Then the orbit of such a solution is $S(x_0) = S_m(x_0) = \{x_0, x_1, \ldots, x_{m-1}\}$, which is an m-periodic orbit of discrete system (4). The initial value x_0 for an m-periodic solution satisfies $x_0 = Q_0^{(m)}(x_0)$, where $Q_0^{(m)}$ is the composition of Q_0 with itself m times.

Let x_n be an m-periodic solution of (4). Pick a solution $x(t)$ of (1)–(3) for $t \geqslant t_0$ with some initial values $t_0 > 0$ and $x(t_0^-) = x_0$. Then $x(t)$ is periodic with the period $T = \Phi(x_0) + \ldots + \Phi(x_{m-1})$ and has exactly m impulses on the periodicity interval $[0,\ T)$. Moreover, $t_m = t_0 + T$. Such a solution $x(t)$ will be called an m-cycle. It follows from Proposition 1 that, for a fixed t_0, system (1)–(3) always has a unique 1-cycle.

An orbit $S(x_0)$ of discrete equation (4) is called asymptotically stable [4] if

(i) for any neighborhood $V \supset S$, there exists a neighborhood $U \supset S$ such that $x_n \in V$ for all $x_0 \in U$ and $n \geqslant 0$;

(ii) there exists a neighborhood $U_0 \supset S$ such that the distance $\mathrm{dist}\,(x_n, S) \to 0$ for all $x_0 \in U_0$, as $n \to \infty$.

For (4), an m-periodic orbit $\{x_0, x_1, \ldots, x_{m-1}\}$ is asymptotically stable if

$$-1 < Q_0'(x_0)Q_0'(x_1)\ldots Q_0'(x_{m-1}) < 1.$$

Since the hybrid system under consideration is of dimension two (one continuous state and one discrete), consider a 2-dimensional orbit (a set of ordered pairs) $S^*(x_0, t_0) = \{(x_n, t_n),\ n = 0, 1, \ldots\}$. Clearly, it is not periodic even in the case when $S(x_0)$ is an m-periodic orbit of (4). Since $t_{n+1} = t_n + \Phi(x_n)$, for an asymptotically stable S, the orbit S^* will not be asymptotically stable. Indeed, small perturbations in t_0 remain small as n increases, but do not vanish.

III. OBSERVER EQUATIONS

The purpose of observation in hybrid system (1)–(3) is to produce estimates $(\hat{t}_n,\ \hat{\gamma}_n)$ which are close (in the sense defined below) to the impulse parameters $(t_n,\ \gamma_n)$. To that end, an observer mimicking the dynamics of the plant is introduced as:

$$\frac{d\hat{x}}{dt} = -\lambda\hat{x} + K(x - \hat{x}), \tag{6}$$

where

$$\hat{x}(\hat{t}_n^+) = \hat{x}(\hat{t}_n^-) + \hat{\gamma}_n, \tag{7}$$

$$\hat{t}_{n+1} = \hat{t}_n + \hat{T}_n, \quad \hat{T}_n = \Phi(\hat{x}(\hat{t}_n^-)), \quad \hat{\gamma}_n = F(\hat{x}(\hat{t}_n^-)) \tag{8}$$

and K is a static feedback gain that is a positive scalar. Without loss of generality, it is assumed that $\hat{t}_0 \geqslant t_0$.

The observer design objective is then to ensure asymptotical convergence of the sequence $\{\hat{t}_n\}$ to $\{t_n\}$, i.e. to synchronize the impulses in the observer with those of the plant by a suitable choice of K.

Since the state $x(t)$ undergoes jumps at certain time instants, the closeness of $x(t)$ and $\hat{x}(t)$ cannot be guaranteed for all t. Indeed, the solutions $x(t)$ and $\hat{x}(t)$ can differ significantly in vicinity of a jump. However, closeness of $x(t)$ and its estimate $\hat{x}(t)$ can be ensured in the sense that there exists a constant integer $a > 0$ depending on initial conditions and such that $\hat{t}_n - t_{n+a} \to 0$ and $|\hat{x}(\hat{t}_n^-) - x(t_{n+a}^-)| \to 0$ as $n \to +\infty$.

Summing up, the overall dynamical system under consideration is the one comprising the plant and the observer and governed by (1)–(3), (6)–(8).

IV. POINTWISE MAPPING AND ITS PROPERTIES

Pick a solution $x(t)$ of plant equations (1)–(3) with the parameters $t_i,\ \gamma_i,\ i = 0, 1, 2, \ldots$. This solution will further be fixed. Consider the sets

$$U_{k,s} = \{\,(x,t)\ :\ t_k \leqslant t < t_{k+1}, \quad t_s \leqslant t + \Phi(x) < t_{s+1}, \\ x, t \in \mathbb{R}^+\,\} \tag{9}$$

for $k = 0, 1\ldots,\ s = k, k+1, \ldots$. For brevity sake, denote $x_k = x(t_k^-)$. It is seen that any sufficiently small neighborhood W_k of a point (x_k, t_k) satisfies the inclusion (see Fig. 1)

$$W_k \subset U_{k,k} \cup U_{k-1,k+1} \cup U_{k-1,k} \cup U_{k,k+1}.$$

For brevity sake, denote $\hat{x}_n = \hat{x}(\hat{t}_n^-)$. Consider the pointwise mapping describing the evolution of the observer state:

$$(\hat{x}_n,\ \hat{t}_n) \mapsto (\hat{x}_{n+1},\ \hat{t}_{n+1}). \tag{10}$$

Define $P(x,t) = P_{k,s}(x,t)$ for $k = 0, 1, \ldots,\ s \geqslant k$, $(x,t) \in U_{k,s}$ with

$$P_{k,s}(x,t) = \mathrm{e}^{-\lambda(t+\Phi(x)-t_s)}x(t_s^+) \\ - \mathrm{e}^{-(\lambda+K)\Phi(x)}\left[\mathrm{e}^{-\lambda(t-t_k)}x(t_k^+) - x - F(x)\right] \\ - \sum_{j=k+1}^{s} \gamma_j e^{-(\lambda+K)(t+\Phi(x)-t_j)}.$$

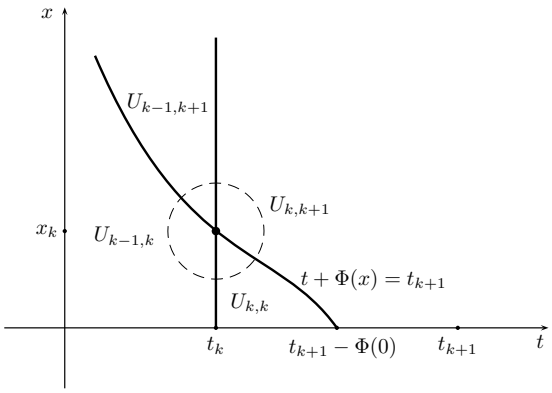

Fig. 1: A neighborhood of the point (x_k, t_k)

Theorem 1: Pointwise mapping (10) is given by the equations

$$\hat{x}_{n+1} = P(\hat{x}_n, \hat{t}_n), \quad \hat{t}_{n+1} = \hat{t}_n + \Phi(\hat{x}_n). \tag{11}$$

Proof: The proof is along the lines of the proof of Theorem 1 in [1]. ∎

Theorem 2: The mapping $P(x,t)$ is continuous.

Proof: Omitted. ∎

Dissimilar to the case previously considered in [1], the mapping $P(x,t)$ is not continuously differentiable (see Theorem 3). This is despite the fact that the scalar plant in (1) is just a specialization of the linear plant treated in [1]. Already for a second-order (and higher) continuous dynamics, all the results in [1] apply. However, as explained below, the case of a scalar plant needs special attention.

For a sufficiently small neighborhood of a point (x_k, t_k), $k \geqslant 1$, the mapping $P(x,t)$ can only take the following values: $P(x,t) = P_{r,s}(x,t)$, where $(x,t) \in U_{r,s}$ and $U_{r,s}$ is one of the four sets $U_{k,k}$, $U_{k-1,k+1}$, $U_{k-1,k}$, $U_{k,k+1}$.

Theorem 3: The partial derivatives of $P(x,t)$ at a point (x_k, t_k), $k \geqslant 1$, can be computed as follows:

$$\begin{aligned}
\tfrac{\partial}{\partial x} P_{k,k}(x_k,t_k) &= -\lambda x_{k+1}\Phi_k' + \mathrm{e}^{-(\lambda+K)T_k}\left(1+F_k'\right),\\
\tfrac{\partial}{\partial t} P_{k,k}(x_k,t_k) &= -\lambda\left(1-\mathrm{e}^{-KT_k}\right)x_{k+1},
\end{aligned}$$

and

$$\begin{aligned}
\tfrac{\partial}{\partial x}\, P_{k-1,k}(x_k,t_k) &= \tfrac{\partial}{\partial x}\, P_{k,k}(x_k,t_k),\\
\tfrac{\partial}{\partial t}\, P_{k-1,k}(x_k,t_k) &= \tfrac{\partial}{\partial t}\, P_{k,k}(x_k,t_k) + K\gamma_k \mathrm{e}^{-(\lambda+K)T_k},\\
\tfrac{\partial}{\partial x} P_{k,k+1}(x_k,t_k) &= \tfrac{\partial}{\partial x} P_{k,k}(x_k,t_k) + K\gamma_{k+1}\Phi_k',\\
\tfrac{\partial}{\partial t} P_{k,k+1}(x_k,t_k) &= \tfrac{\partial}{\partial t} P_{k,k}(x_k,t_k) + K\gamma_{k+1},\\
\tfrac{\partial}{\partial x}\, P_{k-1,k+1}(x_k,t_k) &= \tfrac{\partial}{\partial x}\, P_{k,k+1}(x_k,t_k),\\
\tfrac{\partial}{\partial t}\, P_{k-1,k+1}(x_k,t_k) &= \tfrac{\partial}{\partial t}\, P_{k,k+1}(x_k,t_k) + K\gamma_k \mathrm{e}^{-(\lambda+K)T_k}.
\end{aligned}$$

Proof: Omitted. ∎

Theorem 3 implies that the partial derivatives of $P(x,t)$ have gaps in any neighborhood of (x_k, t_k) on the borders between the regions $U_{u,v}$.

Introduce additional notation pertaining to mapping (10). Define the functions

$$Q_{k,s}(x,t) = \begin{bmatrix} P_{k,s}(x,t) \\ t+\Phi(x) \end{bmatrix}, \quad Q(x,t) = \begin{bmatrix} P(x,t) \\ t+\Phi(x) \end{bmatrix}.$$

Then $Q(x,t) = Q_{k,s}(x,t)$ for $(x,t) \in U_{k,s}$ and

$$\begin{bmatrix} \hat{x}_{n+1} \\ \hat{t}_{n+1} \end{bmatrix} = Q(\hat{x}_n, \hat{t}_n).$$

The Jacobian of $Q(x,t)$ is given by

$$Q'(x,t) = \begin{bmatrix} P_x'(x,t) & P_t'(x,t) \\ \Phi'(x) & 1 \end{bmatrix}$$

at those points (x,t) where the partial derivatives exist.

V. SYNCHRONOUS MODE

Let $(x(t),\, t_n)$ be a solution of plant equations (1)–(3) with the parameters γ_k, T_k, and $x_k = x(t_k^-)$. Suppose that the plant is already running at the moment when the observer is initiated, i.e. $t_a \leqslant \hat{t}_0 < t_{a+1}$ for some $a \geqslant 1$.

Considering the solution $(\hat{x}(t),\, \hat{t}_n)$ of observer equations (6)–(8) subject to the initial conditions

$$\hat{t}_0 = t_a, \qquad \hat{x}(\hat{t}_0^-) = x(t_a^-),$$

yields

$$\hat{x}_n = x_{n+a}, \quad \hat{t}_n = t_{n+a}, \quad \hat{\gamma}_n = \gamma_{n+a}, \quad n = 0,\, 1,\, 2,\, \ldots,$$

and $\hat{x}(t) = x(t)$ for $t \geqslant t_a$. Such a solution $(\hat{x}(t),\, \hat{t}_n)$ will be called *a synchronous mode* with respect to $(x(t),\, t_n)$.

A synchronous mode is called *locally asymptotically stable* [2] if for any solution $(\hat{x}(t),\, \hat{t}_n)$ of (6)–(8) such that the initial estimation errors $|\hat{t}_0 - t_a|$ and $|\hat{x}(\hat{t}_0^-) - x(t_a^-)|$ are sufficiently small, it follows that $\hat{t}_n - t_{n+a} \to 0$ and $\hat{x}(\hat{t}_n^-) - x(t_{n+a}^-) \to 0$ as $n \to \infty$. The latter implies $\hat{\gamma}_n - \gamma_{n+a} \to 0$ as $n \to \infty$.

Due to the biological nature of the underlying observation problem, synchronous modes with respect to stable periodic solutions of the plant are considered. Recall the mapping $P(x,t)$ introduced in the previous section. Since $\hat{t}_n = t_{n+a}$ and $\hat{x}_n = x_{n+a}$ for a synchronous mode, it follows that $(\hat{x}_n, \hat{t}_n) \in U_{n+a,n+a+1}$ and

$$\hat{x}_{n+1} = P_{n+a,n+a+1}(\hat{x}_n,\, \hat{t}_n)$$

for all $n \geqslant 0$. Moreover, a small neighborhood of any point $(\hat{x}_n, \hat{t}_n)$ of the orbit corresponding to a synchronous mode lies at the union of the four sets

$$U_{n_a,n_a} \cup U_{n_a-1,n_a+1} \cup U_{n_a-1,n_a} \cup U_{n_a,n_a+1},$$

where, for brevity, $n_a = n + a$.

Denote also $\Phi_k' = \Phi'(x_k)$, $F_k' = F'(x_k)$ and introduce the Jacobians of the mapping $Q_{m,n}$

$$J_{m,n}(x,t) = \begin{bmatrix} \tfrac{\partial}{\partial x}\, P_{m,n}(x,t) & \tfrac{\partial}{\partial t}\, P_{m,n}(x,t) \\ \Phi'(x) & 1 \end{bmatrix}.$$

Further, consider the Jacobians $J_{k,k+1}$, $J_{k-1,k+1}$, $J_{k,k}$, $J_{k-1,k}$ at the point (x_k, t_k). The arguments (x_k, t_k) will be omitted to save space.

Since the matrices $J_{m,n}$ are of dimension 2×2, their eigenvalues are completely characterized by their traces $\operatorname{tr} J_{m,n}$

and their determinants $\det J_{m,n}$. Namely, the characteristic polynomial of a matrix $J_{m,n}$ is

$$\mathfrak{P}_{m,n}(p) = p^2 - p\ \mathrm{tr}\, J_{m,n} + \det J_{m,n}.$$

Schur stability of a polynomial $\mathfrak{P}_{m,n}(p)$ (all roots lie inside the unit circle) is then equivalent to

$$|\,\mathrm{tr}\, J_{m,n}| - 1 < \det J_{m,n} < 1. \tag{12}$$

By making use of the formulas for the partial derivatives given in Theorem 3 and checking inequalities (12), explicit stability conditions for the matrices $J_{k,k+1}$, $J_{k-1,k+1}$, $J_{k,k}$, $J_{k-1,k}$ are obtained.

Proposition 2: For $k \geqslant 1$ we have

$$\begin{aligned} \mathrm{tr}\, J_{k,k+1} &= \mathrm{tr}\, J_{k-1,k+1}, \\ \mathrm{tr}\, J_{k,k} &= \mathrm{tr}\, J_{k-1,k}, \\ \det J_{k,k+1} &= \det J_{k,k}, \\ \det J_{k-1,k+1} &= \det J_{k-1,k}. \end{aligned}$$

Proof: The result follows from Theorem 3. ■

For large gains K, i.e., $K \to +\infty$, Schur stability conditions for the polynomials $\mathfrak{P}_{k,k+1}$, $\mathfrak{P}_{k-1,k+1}$, $\mathfrak{P}_{k,k}$, $\mathfrak{P}_{k-1,k}$ can be easily obtained. One has

$$\begin{gathered} \mathrm{tr}\, J_{k-1,k} = \mathrm{tr}\, J_{k,k} \to 1 - \lambda x_{k+1} \Phi'_{k+1}, \\ \det J_{k-1,k} \to 0, \quad \det J_{k,k} \to 0 \end{gathered}$$

as $K \to +\infty$. Thus, if the inequality

$$\lambda x_{k+1} \Phi'_{k+1} < 2$$

is satisfied, then the matrices $J_{k-1,k}$, $J_{k,k}$ are Schur stable, i.e., all their eigenvalues lie strictly inside the unit circle. At the same time,

$$\mathrm{tr}\, J_{k-1,k+1} = \mathrm{tr}\, J_{k,k+1} \to +\infty$$

as $K \to +\infty$, so the matrices $J_{k-1,k+1}$, $J_{k,k+1}$ become Schur unstable. This is in contrast with the case of higher dimensions of the continuous part treated in [1], where a sufficiently large observer gain always led to local asymptotic stability. Computer simulations in the next section indicate that for most values of the parameters the estimation error of the observer either vanishes, or remains considerably large, depending on initial states.

VI. SIMULATION EXPERIMENTS WITH STATIC GAIN OBSERVER

For the purpose of simulation, assume specific forms of the functions $\Phi(x)$, $F(x)$ [2] that are known as Hill (sigmoidal) functions and widely used in biological modeling:

$$\Phi(x) = k_1 + k_2 \frac{(x/h)^p}{1 + (x/h)^p},\ F(x) = k_3 + \frac{k_4}{1 + (x/h)^p},$$

where parameters the k_1, k_2, k_3, k_4, h are positive and $p \geqslant 1$ is an integer number.

In biological models, the Hill function order p is kept reasonably low. The following parameter values have been chosen: $k_1 = 40$, $k_2 = 80$, $k_3 = 0.005$, $k_4 = 250$, $h = 2.7$, $p = 4$, $0.003 < \lambda < 0.038$.

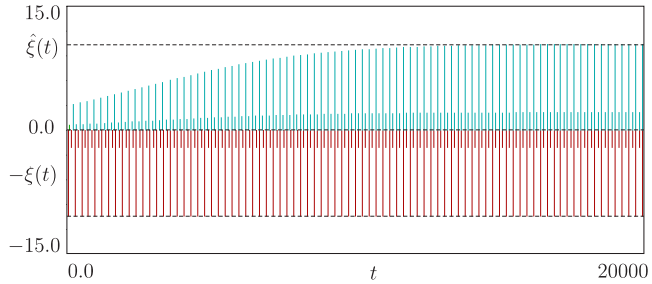

(a)

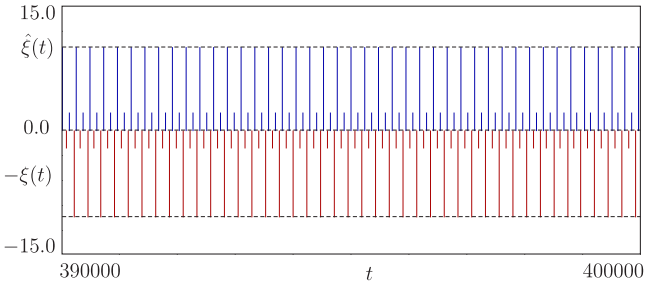

(b)

Fig. 2: Transients in the estimated firing times and amplitudes of the jumps in observer (6) for a 2-cycle ($m = 2$) in the plant. The times and amplitudes (with opposite sign) of the jumps in the plant are plotted in red, $\lambda = 0.0052$, $K = 1.2$. (a) The case of $(\hat{x}_0, \hat{t}_0) \in U_{k,k}$. Synchronization is achieved. (b) The case of $(\hat{x}_0, \hat{t}_0) \in U_{k,k+1}$. Synchronization has failed.

The simulation results confirm the conclusions of Section V. If the initial conditions for observer (6) lie in the regions of stability, a synchronous mode is established after some transient time. If the observer starts in a region of instability, synchronization is never reached.

In Fig. 2 transients in the estimated jump instants and amplitudes are shown for observation of a 2-cycle with the parameters $\lambda = 0.0052$, $K = 1.2$. The light blue lines are positioned at the firing times of the observer $\hat{t}_n$. The red lines are positioned at the jump instants of the plant in the 2-cycle. Here $\xi(t_n) = \gamma_n$, $\hat{\xi}(\hat{t}_n) = \hat{\gamma}_n$ and $\xi(t) = \hat{\xi}(t) = 0$ otherwise. In Fig. 2(a), $(\hat{x}_0, \hat{t}_0) \in U_{k,k}$ (initial conditions in a stability region) and the synchronous mode is achieved in the observer after a transient. In Fig. 2 (b), the observer is initialized so that $(\hat{x}_0, \hat{t}_0) \in U_{k,k+1}$ (initial conditions in an instability region) and synchronization fails. Thus, the observer performance depends on the initialization which effect does not exist in the observers with a higher (than two) order of the continuous part.

However, for initial conditions selected in a stability region, the observer is able to reconstruct signals of a rather high periodicity. For instance, in Fig. 3, a transient to a synchronous mode is depicted for an 8-cycle in the plant with $\lambda = 0.00689$, $K = 1.2$ and $(\hat{x}_0, \hat{t}_0) \in U_{k-1,k}$ (a stability region).

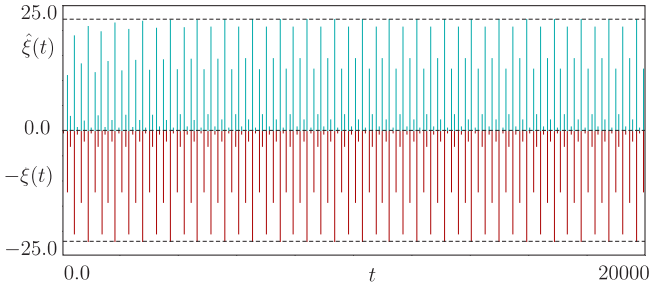

Fig. 3: Transients in the estimated firing times and amplitudes of the jumps in observer (6) for an 8-cycle ($m = 8$) in the plant (in red), $\lambda = 0.00689$, $K = 1.2$ and $(\hat{x}_0, \hat{t}_0) \in U_{k-1,k}$. Synchronization is achieved.

VII. OBSERVER WITH INTEGRATOR FEEDBACK

As follows from the preceding sections, a static gain observer for a first-order system, unlike the one for the multidimensional case, requires a prior search for suitable initial values that makes practical applicability of such an observable debatable. To improve the observer performance, an alternative scheme is suggested, where the state observation error is integrated and then fed back into the plant model of the observer. Thus, instead of (6), the following system is considered

$$\begin{aligned} \frac{dx}{dt} &= -\lambda x + \xi(t), \\ \frac{d\hat{x}}{dt} &= -\lambda \hat{x} + Ky, \quad \frac{dy}{dt} = x - \hat{x}, \end{aligned} \tag{13}$$

where the jumps of $x(t)$ and $\hat{x}(t)$ are described by (2), (3) and (7), (8), respectively, and the third equation describes the observer correction by the integrator output $y(t)$.

Let $\hat{x}_n$ be defined as previously, $\hat{x}_n = \hat{x}(\hat{t}_n^-)$. Introduce a sequence $y_n = y(\hat{t}_n)$. (Notice that $y(t)$ has no jumps.) Consider a mapping

$$(\hat{x}_n, y_n, \hat{t}_n) \mapsto (\hat{x}_{n+1}, y_{n+1}, \hat{t}_{n+1}). \tag{14}$$

Define a matrix D and a column vector B:

$$D = \begin{bmatrix} -\lambda & K \\ -1 & 0 \end{bmatrix}, \quad B = \begin{bmatrix} 1 \\ 0 \end{bmatrix}.$$

Obviously, the matrix D is Hurwitz stable provided that $\lambda > 0$, $K > 0$. Moreover, the eigenvalues of D are real if $\lambda^2 \geqslant 4K$. Let the sets $U_{k,s}$, where $s \geqslant k$, be defined by (9).

Define a vector function $\tilde{P}(x, y, t) = \tilde{P}_{k,s}(x, y, t)$ for $(x, t) \in U_{k,s}$, where

$$\begin{aligned} \tilde{P}_{k,s}(x, y, t) &= \mathrm{e}^{-\lambda(t+\Phi(x)-t_s)} x(t_s^+) B \\ &+ \mathrm{e}^{D\Phi(x)} \begin{bmatrix} x + F(x) - \mathrm{e}^{-\lambda(t-t_k)} x(t_k^+) \\ y \end{bmatrix} \\ &- \sum_{j=k+1}^{s} \gamma_j e^{D(t+\Phi(x)-t_j)} B. \end{aligned}$$

Theorem 4: Pointwise mapping (14) is given by the equations

$$\begin{bmatrix} \hat{x}_{n+1} \\ y_{n+1} \end{bmatrix} = \tilde{P}(\hat{x}_n, y_n, \hat{t}_n), \quad \hat{t}_{n+1} = \hat{t}_n + \Phi(\hat{x}_n). \tag{15}$$

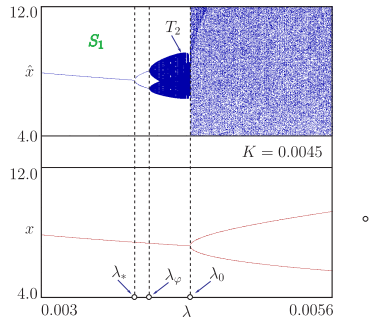

(a)

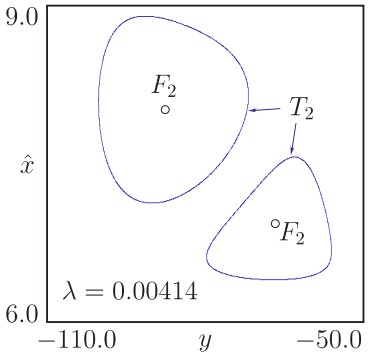

(b)

Fig. 4: (a) Bifurcation diagram for the plant (in red) and for the observer with $K = 0.0045$ (in blue). (b) Two-dimensional projection of the Poincaré section for the observer system after the Andronov-Hopf bifurcation at the point $\lambda = \lambda_\varphi$ in (a), $K = 0.0045$ and $\lambda = 0.00414$. Here T_2 denotes the two-band invariant torus with quasiperiodic dynamics, arising from the asynchronous 2-cycle through an Andronov-Hopf bifurcation at the point λ_φ and F_2 is the the unstable period-2 focus cycle.

and the function $\tilde{P}(x, y, t)$ is continuous.

Proof: Omitted. ■

As in the case of the static-gain observer, partial derivatives of $P(x, y, t)$ in x and in t have gaps at the surfaces $t = t_k$ and $\Phi(x) + t = t_s$. Nevertheless, simulation reveals that for system (13), there exist certain regions of the gain values K that safeguard the observer convergence to a synchronous mode regardless of the initial data. The latter fact indicates global stability of the corresponding solutions. Analytical results to this end are hampered by the discontinuous nature of the derivatives of the pointwise mapping.

Fig. 4 (a) displays the bifurcation diagram illustrating the possible mechanisms of formation of the asynchronous modes in the observer for a fixed observer gain ($K = 0.0045$) and variation of the plant parameter λ. In the interval to the left of the point λ_*, i.e., $\lambda < \lambda_*$, observer (13) displays a stable synchronous 1-cycle. When the increasing λ crosses the point λ_*, an asynchronous 2-cycle is born from the stable 1-cycle synchronous mode through a period-doubling bifurcation.

As the parameter λ increases further, the asynchronous

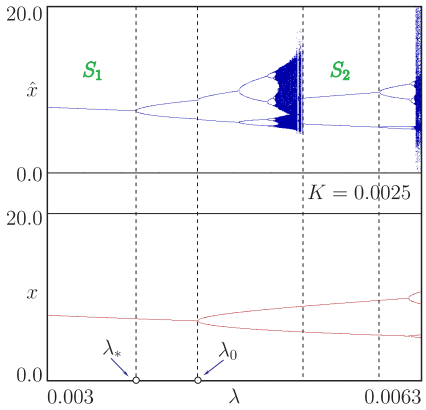

Fig. 5: Bifurcation diagram for the plant (in red) and for the observer with $K = 0.0025$ (in blue). S_1 and S_2 are the regions of existence of the synchronous 1- and 2-cycles, respectively.

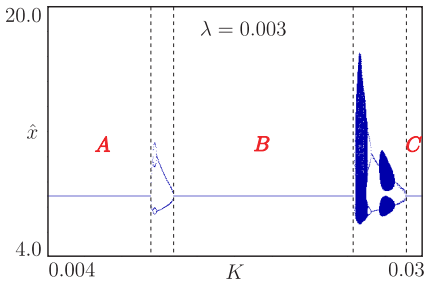

Fig. 6: Bifurcation diagrams for the region of existence of the synchronous 1-cycle, denoted by S_1 in Fig. 5, $\lambda = 0.003$.

2-cycle undergoes an Andronov-Hopf bifurcation [5] at the point $\lambda = \lambda_\varphi$, giving birth to a smooth two-band invariant torus (or a closed invariant curve for the discrete map), that surrounds the asynchronous unstable focus 2-cycle (see Fig. 4 (a)).

Fig. 4 (b) shows the two-dimensional projection of the Poincaré section for hybrid system (13) after the Andronov-Hopf bifurcation, illustrating a smooth two-band invariant torus with quasiperiodic dynamics. Here T_2 denotes the two-band quasiperiodic attractor produced in this bifurcation, and F_2 denotes an unstable focus 2-cycle.

With the further increase of the parameter λ, one can observe the abrupt transition from a stable invariant torus with quasiperiodic dynamics to a chaotic attractor. This transition takes place when the first period-doubling bifurcation point $\lambda = \lambda_0$ is crossed for the plant (Fig. 4 (a)).

The one-dimensional bifurcation diagram in Fig. 5 (for relatively low value of the gain factor $K = 0.0025$) shows the formation of the asynchronous chaotic attractor through an infinite sequence of period-doubling bifurcations for the asynchronous modes.

As illustrated in Fig. 5, the mechanism of formation for a 2-cycle asynchronous mode is the same as the mechanism examined for $K = 0.0045$. A difference only arises in the scenario for the transition to the asynchronous chaos. It is interesting to note, that as the parameter λ increases, one can

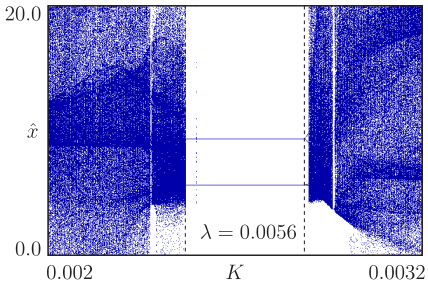

Fig. 7: Bifurcation diagram for the region of the synchronous 2-cycle, denoted by S_2 in Fig. 5, $\lambda = 0.0056$.

observe an abrupt transition from the chaotic attractor to a synchronous 2-cycle.

Fig. 6 shows a one-dimensional bifurcation diagram for a parameter value in the interval $0.003 < \lambda < \lambda_*$, denoted by S_1 in Fig. 5, where the system displays a stable synchronous 1-cycle. With increasing K, one can observe three intervals (denoted by A, B and C) of existence for a stable synchronous 1-cycle, interrupted by regions of asynchronous modes with periodic or aperiodic (chaotic or quasiperiodic) dynamics.

Finally, Fig. 7 shows a one-dimensional bifurcation diagram for the region, denoted by S_2 in Fig. 5, where the system displays a stable synchronous 2-cycle surrounded by regions of chaotic behavior.

VIII. CONCLUSIONS

It is discovered that a static gain observer for the first-order impulsive system has a dramatically different behavior compared to a higher-dimensional one. The ultimate reason for that is the pointwise mapping governing the system dynamics becomes non-smooth in case of scalar continuous part. Thus a lower differential order of the hybrid plant does not result in simplification, but in a substantial complication of the hybrid dynamics of the observer. A possible remedy is foreseen in the introduction of a pure integrator into the feedback of the observer that ensures satisfactory state estimation performance. However, the observer design problem involves intricate bifurcation analysis and specific to the type of the periodic solution of the plant.

REFERENCES

[1] A. Churilov, A. Medvedev, and A. Shepeljavyi, "State observer for continuous oscillating systems under intrinsic pulse-modulated feedback," *Automatica (IFAC journal)*, vol. 48, no. 6, pp. 1005–1224, 2012.

[2] ——, "Mathematical model of non-basal testosterone regulation in the male by pulse modulated feedback," *Automatica*, vol. 45, no. 1, pp. 78–85, 2009.

[3] Z. Zhusubaliyev, A. Churilov, and A. Medvedev, "Complex dynamics and chaos in a scalar linear continuous system with impulsive feedback," in *Proceedings of the 2012 American Control Conference*, Montréal, Canada, June 27 – 29 2012, pp. 2419–2424.

[4] Y. A. Kuznetsov, *Elements of Applied Bifurcation Theory*. New York: Springer–Verlag, 2004.

[5] J. Guckenheimer and P. Holmes, *Nonlinear Oscillations, Dynamical Systems, and Bifurcations of Vector Fields*. New York: Springer-Verlag, 1983.